LOW SWaP MWIR DETECTOR AND VIDEO CORE

G. Gershon [(1)], D. Chen[(1)], R. Gazit[(1)], A. Karabchevsky[(1)], Z. Kiblitski[(1)], O. Magen[(1)], T. Markovitz[(1)], B. Milgrom[(1)], Ilan Nachman[(2)], R. Ohayon[(1)], K. Rozenshein[(1)], N. Syrel[(1)], I. Vladovsky[(1)], M. Weinstein[(1)], and I. Shtrichman[(1)].

[(1)]*SemiConductor Devices (SCD), P.O. Box 2250, Haifa 31021, Israel, Email: galg@scd.co.il.*
[(2)] Ricor, En Harod Ihud 18960, Israel

Keywords: Infrared Detector, HOT, MWIR, XBn, InAsSb, Low SWaP, Video Core, Stirling Cryocooler.

ABSTRACT:

Sparrow is a MWIR detector and video-core module based on SCD's Blackbird 640×512/10µm read-out integrated circuit (ROIC) and it's High Operating Temperature (HOT) XBn-InAsSb Focal Plane Array (FPA). The Sparrow detector enables versatile high-end imaging over a wide spectral range, from the SWIR to the MWIR, and the high FPA operating temperature of 150K allows the use of a low Size, Weight and Power (SWaP) cooler. The Proximity electronics board controls the detector and cooler, and outputs raw video at a frame rate of up to 180Hz. The same board also has thermal imaging video-core capabilities at 60Hz with sub-frame video latency, user-configurable advanced image processing algorithms, and a variety of output video formats. The detector module is equipped with a miniature split-linear Stirling cooler, and a small and stiffened Dewar, which, together with the Proximity electronics board, are compactly harnessed to a low weight metal frame, designed to withstand harsh conditions and allow for easy and efficient integration to the optical system. The module is optimized for a wide range of low SWaP applications, with a volume of 58×62×42 mm^3, a weight of 300g, and a power consumption of 5W at room temperature. In this work we present key results from the Sparrow detector and video-core, which are now in low rate production at SCD.

1. INTRODUCTION

There is growing demand for low SWaP detectors and systems for high-performance MWIR imaging. To meet this need, SCD has developed a 10µm pitch MWIR detector with an array format of 640×512, based on the XBn-InAsSb technology. The digital Read-Out Integrated Circuit (ROIC) exploits an advanced and mature 0.18µm CMOS process and offers high functionality with low power consumption. The 10µm pixel reduces the Focal Plane Array (FPA) footprint and cost, and enables smaller imaging optics, which together with a low Dewar volume and miniature linear cooler, impart a small overall system volume . This creates a very compact thermal imaging video module, with high-end electro-optical performance.

2. ROIC

The Blackbird640 ROIC is part of the Blackbird ROIC family[1], which also includes the Blackbird1280 and Blackbird1920[2] ROICs. It has Analog to Digital Conversion (ADC) at the focal plane, and outputs digital pixel data using LVCMOS or LVDS interfaces. The LVCMOS option is enabled in the Sparrow module, allowing frame rates of up to 180Hz at full frame, and 600Hz with 2×2 binning and low power consumption. For LVDS, a full frame rate of 350Hz is feasible, with over 1000Hz for 2×2 binning.

The ROIC features High Gain mode of 140e^-/DL (0.9Me^- well capacity) with a low readout noise of 250e^-, and Low Gain mode of 300e^-/DL (2Me^- well) with a readout noise of 580e^- at 150K. The two gains are available, both in the IWR (Integrate While Read) mode, and in the ITR (Integrate Then Read) mode that features a 20% reduction in readout noise. Figure 1(a) shows a good linear variation of the squared noise as a function of signal, for different integration times. This result represents a fine readout process for the ROIC pixel, indicating that the detector is Shot-noise limited, and that the readout process does not introduce any additional noise components, such as 1/f, Random Telegraph Signal (RTS) or other phenomena related to various leakage mechanisms, which tend to increase at lower temperatures.

The signal deviation from linearity for different integration-times, is presented in Figure 1(b) as a function of the resultant Well-fill. A low non-linearity of less than 0.04% of the full Dynamic Range (DR) from 5% to 80% capacitor Well-fill demonstrates the linear functionality of the ROIC.

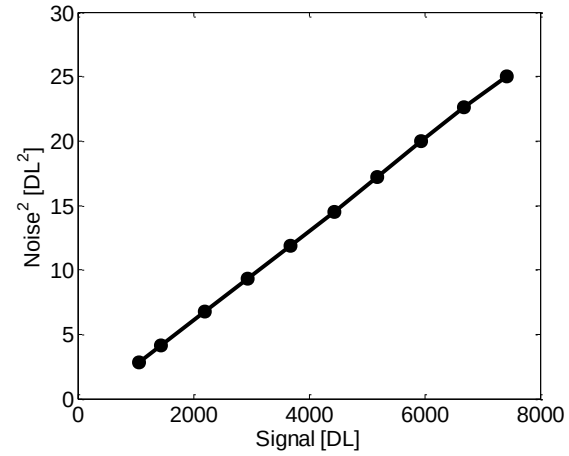

(a)

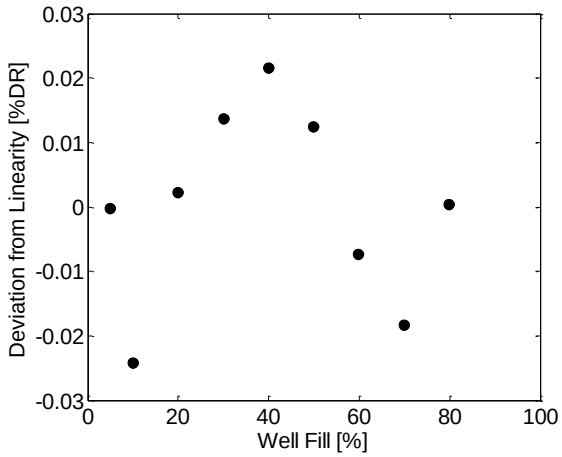

(b)

Figure 1: ***(a)*** *Squared noise as a function of signal in digital levels measured for the Blackbird-640 FPA, for increasing integration times.* ***(b)*** *Deviation from linearity, where the Well-fill is varied using the integration time.*

3. ELECTRO-OPTICAL PERFORMANCE

The main characteristics governing the electro-optical performance of an IR detector are its resolution, sensitivity, uniformity and linear response, and their stability over a wide range of scenarios and environmental conditions. Some are closely related to the performance of the Focal Plane Array (FPA), and some relate to the detector-housing and cooler performance.

SCD has been producing 640×512 and 1280×1024 MWIR detectors with 15µm pitch for more than 10 years, based on the novel XBn-InAsSb barrier detector technology that demonstrates an outstanding electro-optical performance at operating temperatures as high as 150 K[2,3,4], with a cut-off wavelength of 4.2µm covering the "Blue" part of the MWIR spectrum.

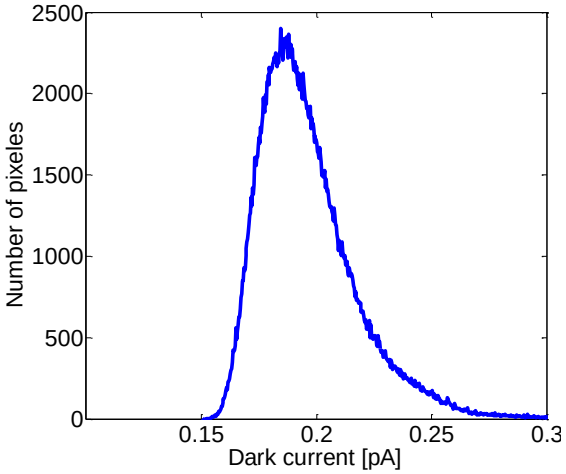

(a)

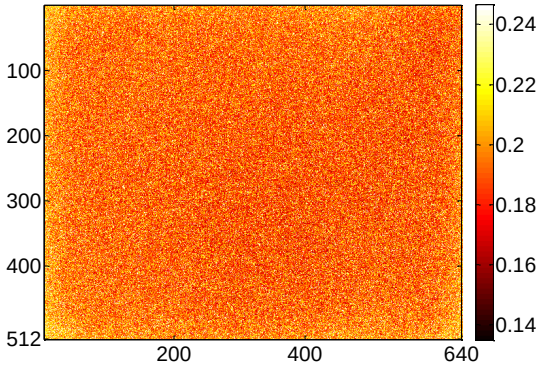

(b)

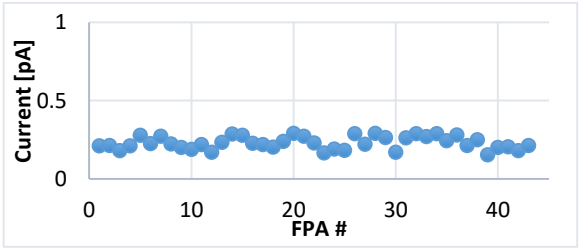

(c)

Figure 2: *Dark current (in pico-Amperes) measured in XBn-InAsSb Blackbird-640 FPA at 150 K and plotted as* ***(a)*** *pixel distribution in the array,* ***(b)*** *2D map,* ***(c)*** *mean values of 45 FPAs from SCD's production line*

To further reduce size, weight, power and cost, SCD has also developed a new XBn pixel with 10µm pitch in a 1280×1024 array format designed for the Blackbird1280 ROIC, and 640×512 format, designed for the new Blackbird 640 ROIC. The XBn array is flip-chip bonded to the ROIC.

The key parameters that determine the performance of the FPA are quantum efficiency (QE) and dark current. High QE and low dark current yield a better temporal signal to noise ratio (SNR), and good signal uniformity reduces spatial noise. Usually in III-V the main contribution to the dark current comes from "Generation–Recombination" (G-R) current that is larger than the "Diffusion" current by several orders of magnitude and has a strong dependence on the FPA temperature. XBn devices are designed to have no depletion zone in the narrow band gap active layer, and hence the G-R current is essentially suppressed. This leaves the much lower Diffusion current, as the dominant source of dark current. In this way it is possible to elevate the operating temperature to 150K with a typical dark current of only 0.2 pA, whose distribution in a typical 640×512 XBn Blackbird FPA is shown in Figure 2(a). The width of the distribution is very narrow, corresponding to a dark current that essentially varies by ~10% across all pixels. Figure 2(b) shows the dark current map of the FPA demonstrating very good spatial uniformity.
The reproducibility of the XBn fabrication process can be seen in Figure 2(c), where a narrow statistical spread exists for the average dark current in 45 FPAs from SCD's Blackbird640 XBn production line.

The measured QE in the XBn FPA is typically 70%, and the MTF is 0.36 at half the Nyquist frequency.

Unlike the dark current and QE, which depend essentially on the photosensitive device alone, other properties can be traced back to a combination of the sensing device and the ROIC. One such property is the detector sensitivity, which is related to the temporal noise of a pixel, and is normally defined by the Noise Equivalent Temperature Difference (NETD). Another two are the uniformity and the linear response of the pixels; both contribute to the residual spatial fixed pattern noise that remains after performing a linear Non Uniformity Correction (NUC). Their effect can be expressed by the Residual Non Uniformity (RNU), which is the maximum standard deviation of all pixels with respect to the NUC linear calibration, at a particular Well-fill.

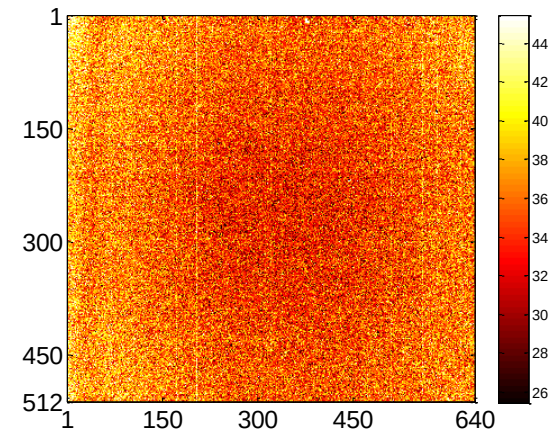

(a)

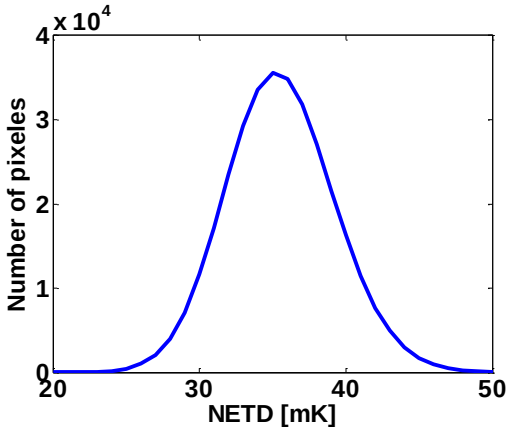

(b)

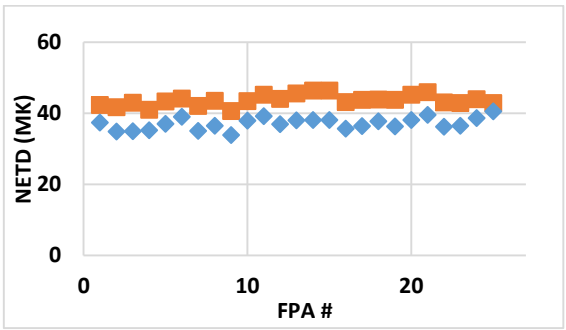

(c)

Figure 3: (a) *Typical NETD image of Blackbird-640 XBn-InAsSb at F/3, 150 K and 30C and 50C blackbody temperature.* ***(b)*** *NETD histogram of the data in Figure 3(a). The average NETD is 36mK and the standard deviation is 4mK.* ***(c)*** *Mean NETD values of 25 FPAs from SCD's production line ATP.*

The NETD at a given frame rate and F/# is one of the critical parameters for the evaluation of an IR detector, and is therefore an important Figure of Merit. It is a measure of the detector's ability to register a temperature difference that creates a signal larger than the noise. Due to the low readout noise and low dark current in Blackbird FPAs, the detector has an NETD corresponding to background limited performance (BLIP) even at low integration capacitor Well-fill (low signal). In Figure 3(a), a typical map of the NETD (per pixel) at 70/50% Well-fill is presented for the 2.0Me⁻ integration mode. As can be seen in the image, there are no spatial features in the temporal noise, indicating no additional noise mechanisms aside from shot noise. In Figure 3(b) a smooth and narrow Gaussian-like histogram is shown for the distribution of the NETD over all FPA pixels. Another example of the good reproducibility of the XBn fabrication process can be seen in Figures 3(c) and 4(c), where a narrow statistical spread exists for the average NETD and RNU as measured during the automated acceptance test procedure (ATP) of more than 25 Sparrow detectors.

The detector uniformity is typically evaluated from an analysis of the corrected image after a NUC procedure. Here we present the RNU measured after a standard linear 2-point NUC, with calibration points at Well-fill levels of 20% and 80% from the full dynamic range (DR). The RNU is inspected for various signal levels corresponding to a wide range of well fills that cover almost the entire DR. When calculated globally for all pixels in the array the RNU is affected by both low and high spatial pattern frequencies in the recorded image, and it is thus termed global RNU. High frequency patterns usually originate from spatial inhomogeneity across nearby FPA pixels. They are related to variations of the parameters of the individual pixels in both the ROIC and the photo-sensitive device, and can often be traced back to the fabrication processes of the two. This type of non-uniformity has white noise characteristics, is local in nature, and determines the ability of the detector to distinguish targets from their close environment.
It is therefore useful to discriminate the high frequency spatial patterns from the low frequency patterns. To that end, we define the Local RNU as the standard deviation (STD) calculated over 15×15 neighbors around a given pixel in the corrected image and averaged for all pixels. As can be seen in Figure 4(a) for the Blackbird640 XBn FPA, it is lower than the global RNU, since low frequency patterns are filtered out.

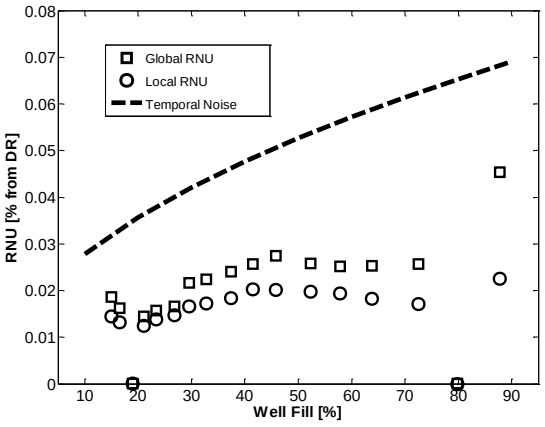

(a)

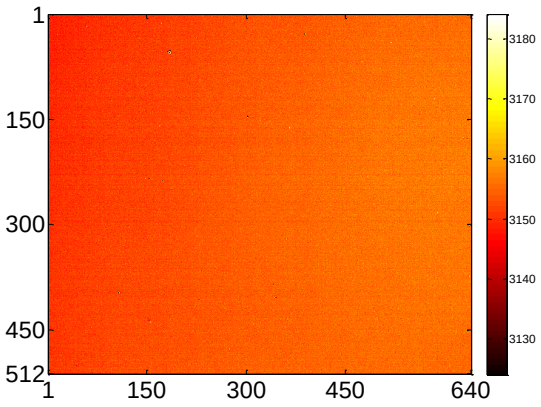

(b)

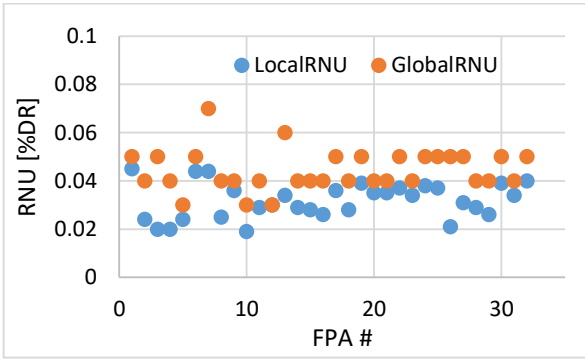

(c)

Figure 4: ***(a)*** *Typical RNU from the Blackbird-640 XBn FPA at F/4, 150 K as a function of Well-fill. The signal is varied by changing the black-body target temperature at constant integration time.* ***(b)*** *An image of a uniform target at 50% Well-fill after 2-point NUC. The color scale is in digital levels.* ***(c)*** *Mean RNU values of 33 FPAs from SCD's production line ATP.*

The global (local) RNU of the Blackbird FPA is less than 0.03% (0.025%) STD/DR for a wide range of signal well fills. A comparison of the spatial noise (RNU) and temporal noise (related to NETD and plotted as a dashed line) in Figure 4(a) indicates the high spatial uniformity of the array.

For a good BLIP detector, the spatial noise should always be significantly lower than the temporal noise, as indeed occurs in Figure 4(a). Figure 4(b) shows a corrected image of a uniform target at 50% Well-fill registered from the XBn FPA of Figure 4(a). The color scale is in digital levels, and shows excellent uniformity at the individual bit-level, consistent with the very low values of RNU in Figure 4(a). Figure 4(b) also demonstrates the very high pixel operability of the FPA, since no Bad Pixel Replacement (BPR) routine is applied.

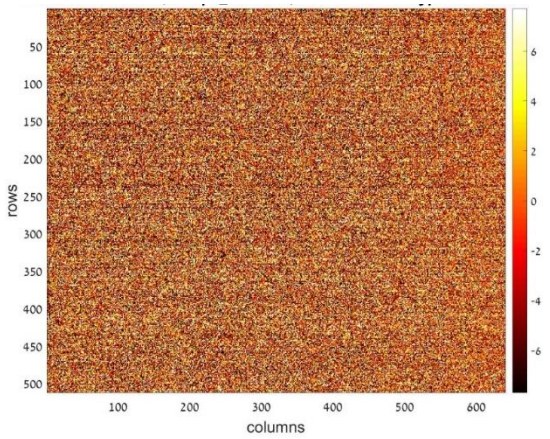

Figure 5: *A typical corrected image with no spatial patterns evident, recorded while the detector is subjected to vibrations*

The detector temporal and spatial noise are also affected by environmental effects such as ambient temperature fluctuations, and mechanical vibrations. Ambient temperature affects the stray light and fluctuations may result in fixed patterns in the corrected image. Mechanical vibrations may cause temporal signal patterns (noise) due to electro-mechanical effects. The stability of the image signal under such harsh conditions is the result of the careful mechanical design and manufacturing of the detector Dewar, while minimizing volume and weight and maintaining high performance. This results in sub-pixel lateral movement of the FPA when the complete integrated detector-cooler assembly (IDCA) is subjected to vigorous vibrations in the frequency range 5-1000Hz. An example for the image stability and endurance to vibrations is presented in Figure 5, where no temporal patterns are evident in the corrected image while the detector is subjected to strong vibrations.

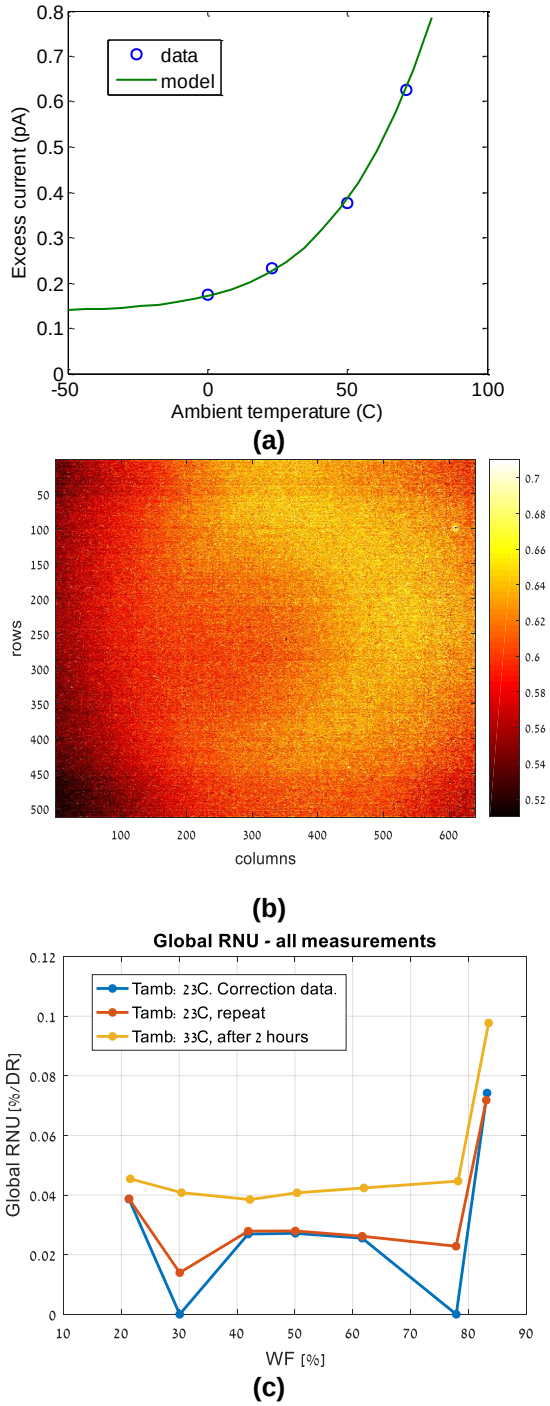

Figure 6: ***(a)*** *Excess Current as a function of ambient temperature (blue circles) and simulated (green line) in a Sparrow IDCA with F#3.0 cold stop* ***(b)*** *Image of the excess current at 71 ℃ ambient* ***(c)*** *Stability of NUC for Sparrow IDCA at different operation times and ambient temperatures.*

The Sparrow IDCA makes a compact MWIR detector that can also withstand harsh environmental conditions such as high ambient temperatures of up to 71 ºC. The design and fabrication of the Dewar minimize the heat load and stray light on the FPA. The Dewar is designed to minimize the Excess Current, namely the sum of the dark current and the photo-current current due to stray light. The excess current in the Sparrow detector as measured in front of a uniform extended blackbody and plotted as a function of the ambient temperature is presented in Figure 6(a). By comparing to an optical model (green line) we conclude that these results correspond to a very low effective emissivity from the surrounding window housing of the Dewar. This good performance of excess current and its uniform nature (Figure 6(b)) impart very stable uniformity of the corrected image even while the ambient temperature is changing. This can be seen also in Figure 6(c), where the global RNU is measured after an ambient temperature change while no update is applied to the NUC tables.

4. CRYOCOOLER

The Sparrow module is equipped with RICOR's new model K590 split-linear Stirling cryo-cooler[6]. The K590 is designed specially to fit SCD's Sparrow video core module requirements. The cryo-cooler is designed for the highest possible compactness, performance, reliability, and for the optimal cost. Generally, the linear compressor concept is the best choice where long life, high efficiency, aural silence, and low vibration levels are required. The K590 dual-opposed linear compressor shown in Figure 7(a) is driven by two “moving magnet” resonant electrodynamic actuators. The actuator topology was optimized for minimal moving components, keeping the highest possible performance and efficiency. The moving magnet actuator assembly is designed to provide the required magnetic spring to the reciprocating parts, allowing better compactness and eliminating use of unreliable and bulky mechanical springs. The “all-welded” compressor case is hermetically sealed by laser welding to provide the highest possible level of sealing reliability. The combination of magnetic springs, a highly efficient motor compressor and an “all welded” case provides a very high level of reliability, ease of assembly and optimal cost for the very low power compressor. The K590 cold head assembly is based on the custom “short” cold finger configuration, and is designed specially to meet SCD's requirements for size, weight and performance in the Sparrow module. The cold head mechanism comprises a pneumatically driven displacer-regenerator assembly, which is attached to a dynamic seals assembly and a mechanical spring. The displacer-regenerator assembly is driven back-and-forth by pressure oscillations coming from the compressor. This motion is required for producing the heat pumping from the expansion space located at the tip of the cold finger, to the warm side at the cold finger base, from which the heat is further dissipated to the environment. The regenerator is shaped as a stack of stainless steel mesh disks of the optimized geometry and porosity.

(a)

Figure 7: (a) *RICOR K590 miniature cooler*

The typical performance of the K590 cryo-cooler at the current project phase is shown in Table 1. The Sparrow module design is compatible also with AIM SX020 cooler which is a single piston split linear cooler.

Table 1. Typical K590 performance

Parameter	Typical Value
Maximum cooling capacity	500mW @ 150K, 71°C
Maximum Input Power	9 W AC
Nominal total heat load	180mW @150K 23°C
Steady State Power	1.8 W AC
Cool down time	2:00 min, 180J @150K ,23°C
Induced vibration force	450 mN rms
Ambient Temperature Range	-40˚C to +71˚C.
MTTF	>30,000 hours (goal)
Weight	170 gr

5. VIDEO CORE IMAGE PROCESSING

The image processing channel of the Sparrow Imager is divided into image correction and image enhancement sub-systems as shown in Figure 8(a). The subsystems are based on SCD proprietary image processing protocols[7,8,9]. The image correction subsystem deals with raw detector data processing as well as image artifacts, and includes the following algorithms.

- Automatic detector Gain and Exposure Control (AGC+AEC)
- Integration time based Non-Uniformity Correction (NUC)
- Bad Pixel Correction (BPR)
- Noise Reduction in the spatial and temporal domains (NR)

The video generated by the Image correction subsystem is suitable for automated video analysis (Machine vision) while the optional Image enhancement subsystem improves the perceived image for a human observer.

5.1 Image correction subsystem

The image correction subsystems implement a video pipeline that applies a series of algorithms to optimize detector performance, reduce residual non-uniformity (RNU), replace defective pixels and reduce image noise.

AGC/AEC Algorithms

An optional Automatic Gain Control (AGC) algorithm selects the best mode of operation (Low Gain or High Gain) based on the scene radiation conditions while the Automatic Exposure Algorithm (AEC) dynamically adjusts the detector integration time to an optimal value.

Non Uniformity Correction (NUC)

The Sparrow video core implements a time based NUC which modifies the NUC coefficients in real time, as a function of the detector integration time providing superior performance compared with a fixed NUC, as demonstrated in Figure 8(b). NUC coefficient acquisition is embedded in the Sparrow Imager, allowing the user to acquire NUC data to the module at the system level without any external capturing mechanism. The Sparrow Imager supports a multiple NUC tables feature. The user can calibrate up to 10 sets of NUC tables per each detector gain mode (up to a total of 20 sets which is useful in case of multiple system setups, e.g. multiple FOVs, multiple ambient temperature ranges and multiple integration times (in case of a fixed NUC).

The integration time can be updated automatically by the AEC algorithm or manually by the user. There is an option of instant RNU reduction by applying a "One-Point" NUC. In such case, NUC coefficients are updated based on a reference image which is taken against uniform scenery (shutter, optics cover or defocused optics). Such a feature is useful, for example, in the case of optics focus / Field Of View (FOV) change.

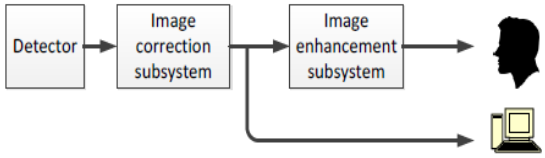

(a)

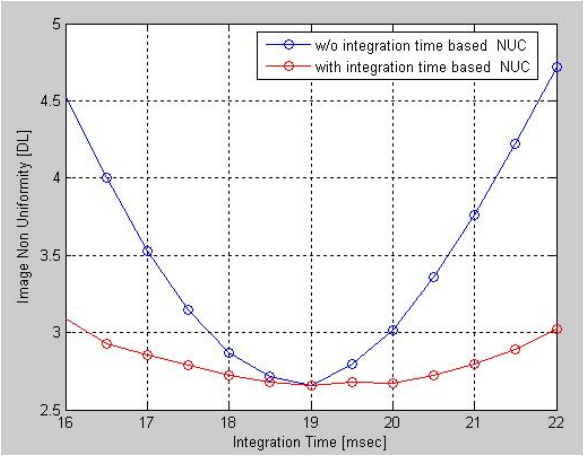

(b)

Figure 8: (a) *Image correction and enhancement sub-systems in Sparrow Imager.* ***(b)*** *Sparrow Imager NUC Performance.*

Bad Pixel Replacement (BPR)

The BPR algorithm uses a preloaded list of bad pixels to replace all bad pixels in the output image, with good pixels generated using a smart edge

reserving, weighted average of adjacent good pixels.

(a)

(b)

Figure 9: *DRC Performance-* ***(a)*** *Linear DRC,* ***(b)*** *Sparrow Imager DRC.*

Noise reduction (NR)

The Sparrow imager implements a proprietary Spatial-Temporal noise reduction algorithm. The NR algorithm uses a combination of spatial and temporal filtering according to inter-frame similarity. The algorithm preserves a maximum level of detail without smearing moving objects in the scene, while maintaining uniform noise levels across the frame and yielding ~×2 temporal noise level reduction.

5.2 Image enhancement subsystem

The image enhancement subsystem is an optional block that improves the perceived image for a human observer and converts the image to the dynamic range of a display – typically 8 bits (256 color levels). The Image enhancement processing includes:

- Dynamic Range Compression (DRC)
- Digital zoom
- Graphics and Overlay
- Pseudo coloring

Dynamic Range Compression (DRC)

DRC performs locally adaptive image contrast enhancement and compresses a 13-bit signal to a displayable 8-bit signal. Both enhancement and compression algorithms are adaptive to scene content. This mechanism ensures maximum contrast enhancement, regardless of input dynamic range variability and overstretching prevention. DRC performance is shown in Figure 9.

Digital Zoom

The Sparrow Imager implements a user configurable ×2 and ×4 digital zoom around the center of the image.

Overlay graphics and Pseudo colors

The Image enhancement subsystem implements graphics and an overlay engine that allows overlaying multiple image graphics stored in the device nonvolatile memory as well as arbitrary text over the Sparrow imager video. Any area in an image painted in a transparent color code is replaced by live video. SCD provides its customers a PC based tool that allows the system integrator to upload images and fonts easily to the device memory. The graphics engine supports simultaneous displaying of up to 15 different colors with a user configurable color palette. In addition, the Sparrow imager data can be converted from gray-color to color space using a pseudo coloring, user configurable look-up table mechanism.

6. SPARROW MODULE SPECIFICATIONS

The Sparrow Dewar-Detector-Cooler-Electronics (DDCE) module is an electro-optical assembly, which converts infrared radiant energy in the MWIR spectral region to video output. There are two mechanical DDCE module configurations compatible with the same mechanical and electrical interface for the Ricor and AIM cryo-

coolers, which are based on the following building blocks:

- XBn-InAsSb detector array with 640×512 format and 10µm pitch.
- On-focal-plane signals processing electronics (ROIC).
- Low SWaP split linear cooler.
- Dewar based on Ricor K590 short cold finger or AIM 5mm cold finger.
- Low weight aluminum frame.
- Electronics – SCD Proxy / Video Engine card with Cooler driver card (both coolers).

The main Sparrow specifications are detailed in Table **1**.

Table 1. Sparrow module specifications

Parameter	Typical Value
Detector Format	640×512, 10µm pixel
Sensing Material	XBn operating at 150K
Integration Modes	ITR, IWR
Integration Capacitors	0.9Me-, 2.0Me-
Operation Modes	Full Image Processing Mode (Video Engine) Raw Digital output (Proxy Mode)
Video Engine Main Processing Algorithms	NUC, BPR, Image Enhancement and DRC, Digital Zoom, Pseudo color, Graphics overlay
Maximum Frame Rate	60 Hz with Image Processing 180Hz without Image Processing
Digital video Resolution	13 bit
NETD (2Me-)	28mK @ 50% well-fill
Residual Non Uniformity	<0.08% STD/DR at 20-80% well-fill capacity
Operability	>99.5%
IDCA Optical Parameters	F/3.6 (standard) Spectral Range:3.6÷4.2µm
Cooler Type	Split Linear
Module MTTF	>18,000 hours (GM @35˚C)
Module Total Power Consumption @23˚C	Typical 4W not including Image Processing Additional 1WDC for full video processing
Image Ready @23˚C	2 minutes (typical)
Module Dimensions	58 × 62 × 42 mm (2.28" × 2.44" × 1.65")
Module Weight	300 gm. (0.66 lb.)

7. SYSTEM ELECTRICAL INTERFACE

The Sparrow Imager is equipped with a single voltage supply proximity electronics card that operates the FPA and cooler, performs the video core image processing, and provides two video channels simultaneously, a parallel video channel and a Camera-Link LVDS video channel, where the LVDS channel can be disabled to reduce power consumption. The parallel video channel is field configured to provide data via a BT656 protocol, a parallel LVCMOS protocol or an AMOLED display mode. The video core provides up to 8 signals referred to as discrete I/O pins that each can be field configured to trigger a specified functionality. The functions, assigned to each discrete I/O pin, are defined by a user changeable control file. Some of the potential signals that can be assigned to the discrete I/O pins are: Black hot / White hot, Digital zoom, One-Point NUC, etc. The Sparrow Imager supports an option for transmitting or receiving a frame synchronization pulse on EXT_SYNC. This feature provides the capability to synchronize frame start with other video sources, an external light pulse source, etc. The video core is controlled by an asynchronous serial interface.

8. SUMMARY

In this paper we presented the "Sparrow", a state-of-the-art Low SWaP MWIR miniaturized video core module. The module consists of a 640×512 XBn-InAsSb FPA operating at 150K coupled to a linear cryo-cooler. We have provided measured electro-optical performance results and described in detail the image processing algorithms that are implemented in the video core.

9. ACKNOWLEDGEMENTS

The development of the Sparrow video core and the BlackBird-640 detector was supported by the Israel Innovation Authority.

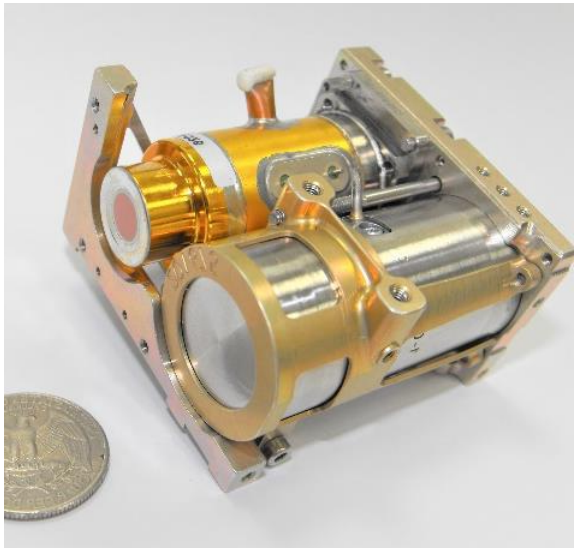

(a)

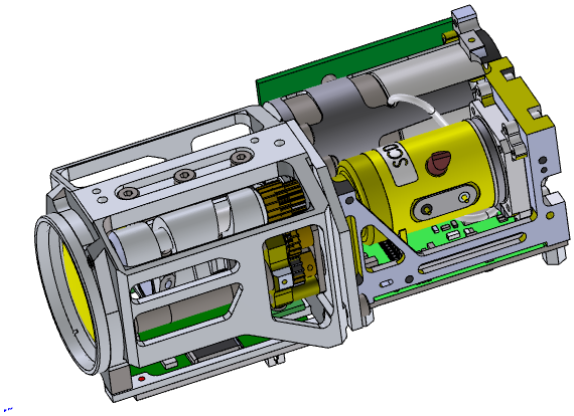

(b)

Figure 10: ***(a)*** *Sparrow module and* ***(b)*** *integrated with optical assembly.*

10. REFERENCES

[1] G. Gershon, E. Avnon, M. Brumer, W. Freiman, Y. Karni, T. Niderman, O. Ofer, T. Rosenstock, D. Seref, N. Shiloah, L. Shkedy, R. Tessler, and I. Shtrichman. "10µm pitch family of InSb and XBn detectors for MWIR imaging". Proc. SPIE 10177, 10177-1I (2017).

[2] G. Gershon, A. Albo, M. Eylon, O. Cohen, Z. Calahorra , M. Brumer, M. Nitzani , E. Avnon, Y. Aghion, I. Kogan, E. Ilan , A. Tuito , M. Ben Ezra and L. Shkedy " LARGE FORMAT InSb INFRARED DETECTOR WITH 10 µm PIXELS". Proc. OPTRO-2014-2931891.

[3] P.C. Klipstein, O. Klin, S. Grossman, N. Snapi, B. Yaakobovitz, M. Brumer, I. Lukomsky, D. Aronov, M. Yassen, B. Yofis, A. Glozman, T. Fishman, E. Berkowicz, O. Magen, I. Shtrichman, and E. Weiss, "XBn Barrier Detectors for High Operating Temperatures", Proc. SPIE 7608, 7608-1V (2010)

[4] I. Shtrichman, D. Aronov, M. ben Ezra, I. Barkai, E. Berkowicz, M. Brumer, R. Fraenkel, A. Glozman, S. Grossman, E. Jacobsohn, O. Klin, P.C. Klipstein, I. Lukomsky, L. Shkedy, N. Snapi, M. Yassen and E. Weiss, "High Operating Temperature epi-InSb and XBn-InAsSb photodetectors" Proc. SPIE 8353, 8353-2Y (2012)

[5] P.C. Klipstein, Y. Gross, D. Aronov, M. ben Ezra, E. Berkowicz, Y. Cohen, R. Frenkel, A. Glozman, S. Grossman, O. Klin, I. Lukomsky, T. Markowitz, L. Shkedy, I. Shtrichman, N. Snapi, A. Tuito, M. Yassen, and E. Weiss " Low SWaP MWIR detector based on XBn Focal Plane Array", Proc. SPIE 8704, 8704-1S (2012).

[6] Sergey Riabzev, Dmitry Radchenko, Dror Raf, Ilan Nachman, Sergey Sobol, Dan Gover, “RICOR’s new development of HOT cryocoolers: compact cost-effective linear model", SPIE 2019

[7] Y. Shamay, E. Braunstain, R. Gazit, Y. Gridish, R. Iosevich, S. Linzer Horesh, Y. Lury, R. Meshorer, U. Mizrahi, E. Raz, M. Savchenko, N. Syrel, S. Yuval, “Low SWaP 640× 480/17µm Uncooled Detector and Video Core.” (Optro 2016).

[8] I. Hirsh, E. Louzon, A. Aharon, R. Gazit, D.E. Bar, P. Kondrashov, M. Weinstein, M. Savchenko, M. Regensburger, A. Navon, E. Shunam, O. Rahat, A. Mediouni, E. Mor, A. Shay, R. Iosevich, M. Ben-Ezra, A. Tuito and I. Shtrichman, "Low SWaP SWIR video engine for image intensifier replacement." Proc. SPIE 10624, 10624-06 (2018).

[9] Rotem Gazit , Alexander Karabchevsky , Dan Chen , Gal Gershon , Irena Vladovsky , Itay Shtrichman , Kobi Rozenshein , Moshe Weinstein , Nickolay Syrel , Omer Rozenberg , Osnat Magen , Roei Ohayon , Sergey Riabzev, Tuvy Markovitz , Zohar Kiblitski. " Low SWaP video core for MWIR imaging" Proc. SPIE 11002/110021 (2019).